

CATARSIS: Calar Alto "Tetra-ARmed Super-Ifu Spectrograph" Survey

Sánchez-Blázquez, P.¹, Gil de Paz, A.¹, Iglesias, J.², Oñorbe, J.³, Montaña, A.⁴, Kehrig, C.², and TARSIS Consortium and instrument team, and CATARSIS team

¹ Departamento de Física de la Tierra y Astrofísica, Fac. CC. Físicas, & Instituto de Física de Partículas y del Cosmos, IPARCOS-UCM, Universidad Complutense de Madrid, Plaza de las Ciencias 1, Madrid, Spain

² Instituto de Astrofísica de Andalucía (CSIC), Apdo. 3004, E-18008, Granada, Spain

³ Facultad de Físicas, Universidad de Sevilla, Avda. Reina Mercedes s/n. Campus Reina Mercedes. E-41012, Seville, Spain

⁴ Instituto Nacional de Astrofísica, Óptica y Electrónica, Luis Enrique Erro No. 1, C.P. 72840, Tonantzintla, Puebla, Mexico

Abstract

The Calar Alto Tetra-Armed Super-IFU spectrograph Survey, CATARSIS, is the new legacy survey for the 3.5m telescope at the Calar Alto Observatory using an integral field spectrograph with a field of view 2.8×2.8 arcmin (TARSIS). The survey will address questions in ambits that go from the fundamental physics and cosmology to the stellar nucleosynthesis, including, but not limited to the study of dark matter and energy nature, the growth of cosmological structures or the evolution of galaxies in them and the evolution of the Ly α function during the epoch

1 Introduction

CATARSIS will use 600 nights to obtain 2D spectra of 16 galaxy clusters at redshifts $0.15 < z < 0.2$ using a new instrument, TARSIS (Tetra ARmed Super-Ifu Spectrograph, Gil de Paz in this proceedings). The clusters will be mapped to a distance of $\sim 2R_{200}$, with an average of 42.1 pointings per cluster and 2 arcsec resolution. Long exposures (~ 8 h per pointing) will provide spectra in the range 320-810 nm for targets with a surface brightness $\mu_r \leq 23.6$ mag/arcsec² (see Fig. 1).

There are two major far-reaching interests that motivate our understanding of the population of galaxy clusters. Firstly, they are ideal test objects to check the likelihood of a given

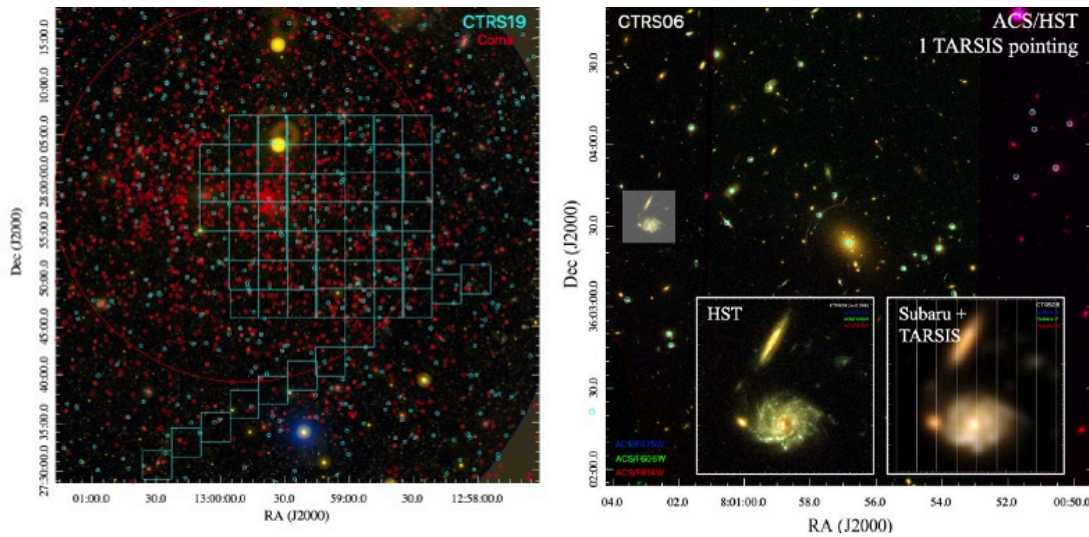


Figure 1: Left panel: Planned mapping for CTRS19. This cluster is located at $z=0.158$, near the approximate coordinates of the Coma cluster, which is at $z=0.023$. This mapping simultaneously covers a large part of the Coma cluster up to its R_{500} (red circle). Confirmed members of CTRS19 are marked in cyan, while galaxies belonging to Coma are marked in red. The projected mosaic with TARSIS is shown in cyan. Right panel: Hubble Space Telescope image of the central region of cluster CTRS6, corresponding to a single TARSIS pointing. Some of the features in this image correspond to background galaxies that are magnified and distorted by the gravitational lensing effect. The details included at the bottom show two of the objects seen by HST and an image obtained from the ground, degraded to the effective resolution of CATARSIS data.

cosmological model to describe our Universe; secondly, they are very important probes of the astrophysical and chemical evolution of the baryonic component of the Universe ([15]; [12]).

In recent years, spectroscopic observations of large sample of galaxies in nearby clusters have become possible due to the advent of CCD mosaics and high multiplex multi-object fiber-fed spectrographs (MOS) (eg, [17]; [8]). However, MOS observations have two main limitations for the study of the cluster structure and the evolution of galaxies: (1) targets need to be pre-selected in advance, which commonly results in spatial and colour biases that turn into biases in the velocity distribution; (2) spectral information is reduced to a given aperture, which does not allow to capture the transformation of galaxies when they first fall into the cluster, which usually start in the external parts.

The selected clusters have abundant archival data in their central regions. Furthermore, complementary observations with the Large Millimeter Telescope (LMT) TolTec camera (<http://toltec.astro.umass.edu/about.php>), will be used to measure the thermal structure of the intracluster medium (ICM) and the non-thermal motions via Sunyaev-Zeldovich effect with $6''$ resolutions. This analysis will result in a much deeper understanding of the galaxy cluster physics which, in turn, will allow calibrating the observations of ongoing or future statistical surveys.

Furthermore, being a blind survey, CATARSIS has an important component of serendipitous science related to galaxies at high redshift. Due to the long exposure times, the large field of view (FoV) of TARSIS and its wavelength coverage, CATARSIS will be very competitive in the detection of high-redshift targets and, in particular, in the detection of Lyman- α emission at redshifts $1.63 < z < 3$, even when compared to other surveys using instruments in 8-m class telescopes.

2 Galaxy Clusters as Cosmological probes

In the standard parametrization of the cosmological model, where the universe contains dark energy, cold dark matter, and ordinary matter, the Λ CDM paradigm, dark matter halos grow hierarchically through accretion of neighbouring substructures. Most massive halos, corresponding to galaxy clusters, form latest ([4];[6]), and are also the most dynamically immature. Preferentially located at the nodes of the complex filamentary web, clusters are continually accreting dark matter halos containing individual galaxies or galaxy groups, and they are unique laboratories for studying the non-linear evolution of the universe. A good understanding and observational characterisation of galaxy clusters, their structure and dynamical state is required to attain these goals.

The large number of redshifts, the area coverage and the lack of spatial biases in the sample of galaxies observed by CATARSIS will allow the characterization of cluster substructure, shape and velocity anisotropies. These measurements will help to reduce the uncertainties in the determination of density profiles with kinematic ([11]) and weak gravitational lensing methods, and it will enable the measurement of the mass accretion rates, the dark matter self interaction, the Universe's expansion rate at the cluster redshifts, and the spectrum of primordial density fluctuations, among others.

3 Evolution of galaxies in clusters

CATARSIS will also improve our understanding of galaxy transformations in clusters. Observations have shown that the morphological mix and the star formation rate (SFR) of galaxies in clusters strongly evolve with redshift ([13]; [5]; [7]). Different processes are capable of transforming galaxy properties when they enter a galaxy cluster ([9]): repeated rapid encounters with other galaxies (harassment), removal and thermal heating of the interstellar medium by the ram-pressure ([14]), or removal of hot gas reservoirs from galaxy halos (strangulation, [10]), are some of them. These mechanisms shape the galaxy evolution in different timescales (from 100 Myr to 1 Gyr), and with different efficiency depending on the properties of both, galaxies and clusters, and the circumstances under which infall takes place ([3]; [2]). Diagnostics of the star formation rate depend on the photoionization of massive stars and thus reflect activity only over the past 5–10 million years, after which photoionization declines rapidly. Studies of stellar populations in the optical range are also unable to distinguish whether star formation ceased a thousand or a hundred million years ago if the mass of young stars represents only a small percentage of the total mass. However, at wavelengths below 300 nm, it

is possible to detect residual star formation that represents as little as 1% of the mass ([16]) (see Fig. 2). The rest-frame spectral range of galaxies in the CATARSIS clusters at $z=0.15$ (278–704 nm) and $z=0.23$ (260–658 nm) will thus allow us to characterize the timescales over which galaxies quench as a function of cluster entry epoch, substructure membership, and the thermodynamic properties of the gas.

Furthermore, galaxy transformations usually start in the outskirts of galaxies, with lower binding energy (see Fig. 2), process that will be capture by CATARSIS observations.

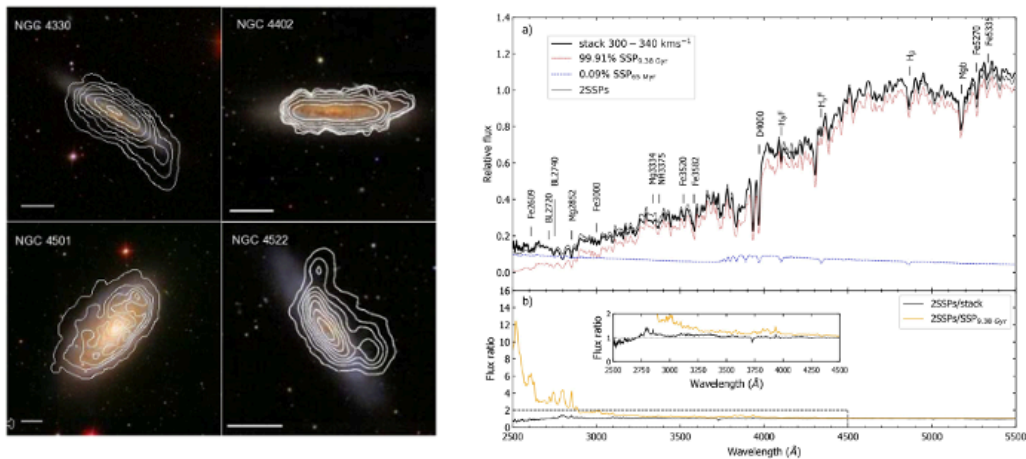


Figure 2: Left panel: False-color SDSS images of galaxies falling into the Virgo cluster. The HI emission (coming from the VIVA survey; Chung et al. 2009) is indicated with the white contours, showing the neutral gas of the galaxy is being stripped from outside-in. Right panel: Top: UV-optical SED of two stellar populations, one Simple Stellar Population (SSP) of 10 Gyr (in black) and one SSP with a 0.01% (in mass) young burst (63 Myr-old, in red). Bottom: Ratio between the two models. Note that only in the UV range the two spectra show significant differences.

4 Behind the clusters

Our deep exposures will serendipitously observe a large variety of different objects at high redshifts and, thanks to its blue coverage, the current MUSE redshift desert at redshifts $1.5 \leq z \leq 3$ (corresponding to the redshift of $[\text{O II}]\lambda\lambda 3726, 3729\text{\AA}$ emitters at the red end and of Ly α Emitters (LAE) at the blue end) will be largely filled down to $z = 1.63$ by CATARSIS (see Fig. 3). Among other things, this will allow us to better characterize the nature Damped Lyman Alpha systems (DLA), $[\text{OII}]$, HeII or Ly α emitters. We will be able to observe Ly α and MgII emission at the same time in objects between $1.63 < z < 1.9$, which will be a giant step to understand the resonance nature of both lines and to quantify the Ly α escape fraction. Furthermore, our detection limit will allow the study of the intergalactic medium emission and, therefore, to understand better the physics of gas inflows and outflows. CATARSIS will provide new ways of exploring the physics associated to high-redshift objects allowing the

same study to be done at much lower redshifts. Although these projects are normally carried out in large aperture telescopes, the large field of view, the much smaller cosmic dimming, and the efficiency of TARSIS make this project highly competitive. Using the Ultra-Fast Image Generator for wide astronomy surveys ([1]) and a limiting magnitude of $r = 22$ mag, we calculate that the number of galaxies observed serendipitously will be 8000 to 9000 per square degree. This adds up to a total of 12000-15300 spectra at the end of the survey. The detection of galaxies with strong emission lines will more than triple this number.

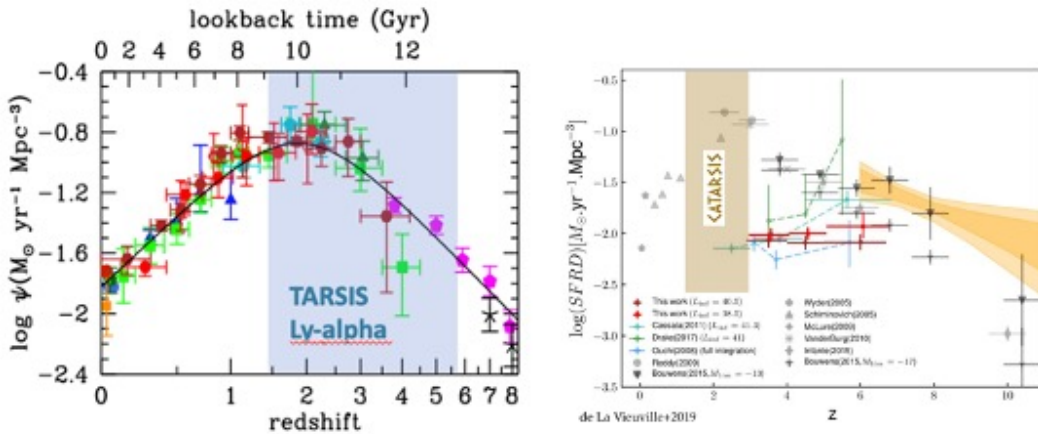


Figure 3: Left: Cosmic SFR density as a function of redshift (the Cosmic Noon is seen between $1.5 < z < 3$). Right: Evolution of the star formation rate density for LAE (de La Vieuville et al. 2019).

5 Summary

The CATARSIS survey will make significant contributions to our understanding of structure formation and galaxy evolution in dense environments. Observations with TARSIS offer two major advantages over other spectroscopy surveys of galaxy clusters: (1) targets do not need to be pre-selected, eliminating biases related to spatial position, color, or brightness of galaxies; and (2) it provides 2D spectra, enabling more detailed studies of galaxy transformations. Additionally, the broad wavelength coverage allows the detection of residual star formation at extremely low levels, the observation of the $\text{Ly}\alpha$ line emitted by objects at redshifts between 1.6 and 3.2, and detailed investigations of DLAs, HeII, and LAEs during the peak of cosmic star formation.

The unique capabilities of TARSIS will also support a variety of other studies, ensuring the scientific productivity of the CAHA observatory for years to come.

Acknowledgments

This work has been funded by the Spanish Ministerio de Ciencia e Innovación (MCIN) and the Agencia Estatal de Investigación (AEI) under the projects PID2022-138855NB-C31 and PID2022-138621NB-

I00. We also wish to acknowledge the financial support from the program Tecnologías Avanzadas para la Exploración del Universo y sus Componentes (TAU-CM).

References

- [1] Bergé, J.; Gamper, L.; Réfrégier, A.; Amara, A., 2013, *A&C*, 1, 23
- [2] Berrier, J. C.; Stewart, K. R.; Bullock, J. S.; Purcell, C. W.; Barton, E. J.; Wechsler, R. H.
- [3] Boselli, A.; Gavazzi, G., 2006, *PASP*, 118, 517
- [4] Boylan-Kolchin, M.; Springel, V.; White, S.D. M.; Jenkins, A.; Lemson, G.
- [5] Dressler, A., 1980, *ApJ*, 236, 351
- [6] Gao, L.; Navarro, J. F.; Frenk, C. S., et al., 2012, *MNRAS*, 425, 2169
- [7] Fasano, G.; Poggianti, B. M.; Couch, W. J., et al., 2000, *ApJ*, 542, 673
- [8] Fasano, G.; Marmo, C.; Varela, J. et al., 2006, *A&A*, 445, 805
- [9] Haines, C. P.; Gargiulo, A.; La Barbera, F., et al., 2007, *MNRAS*, 381, 7
- [10] Kawata D., Mulchaey, J.S., 2008, *ApJ*, 672, 103
- [11] Logan, C. H. A.; Maughan, B. J.; Diaferio, A., et al., 2022, *A&A*, 665, 124
- [12] Mantz, A.; Allen, S. W.; Ebeling, H.; Rapetti, D., 2008, *MNRAS*, 387, 1179
- [13] Oemler, Augustus, Jr., 1974, *ApJ*, 194, 1
- [14] Quilis, V.; Planelles, S.; Ricciardelli, E., 2017, *MNRAS*, 469,80
- [15] Rosati, P.; Borgani, S.; Norman, C., 2002, *ARA&A*, 40, 539
- [16] Salvador-Rusiñol, N.; Vazdekis, A.; La Barbera, F., et al. , 2020, *NatAs*, 4, 252
- [17] Smith, R. E.; Dahle, H.; Maddox, S. J.; Lilje, P. B., 2004, *ApJ*, 617, 811